

# Adult-Size Humanoid Robot Throwing the First Pitch at a Major League Baseball Game

## A Road Map

Daniel M. Lofaro  
Electrical and Computer Engineering  
Drexel University  
Philadelphia, PA, USA  
Email: dan@danLofaro.com

Paul Oh  
Mechanical Engineering  
Drexel University  
Philadelphia, PA, USA  
Email: paul@coe.drexel.edu

**Abstract**—Three different approaches of having an adult-size humanoid robot throw the first pitch at a Major League Baseball game are tested and implemented. The approaches include kinematic mapping using a motion capture system to capture a human’s throwing motion then mapping that to an adult-size humanoid robot. The second method is a fully automated approach that uses the sparse reachable map to provide viable full body throwing trajectories to provide the end effector with the desired velocity. The third approach borrows from the animation industry. Key-frames of the desired trajectory is constructed by hand. The time between each key-frame is defined by the user. Interpolation methods are used to smoothly move between key frames while limiting the jerk. Each method is analyzed and tested in simulation and on physical hardware. The adult-size humanoid robot used is the Hubo series robot. Based on the latter tests one method was chosen to successfully throw the ceremonial first pitch at a Major League Baseball game in April 2012.

### I. INTRODUCTION

In early February 2012 the director of the Philadelphia Science Festival asked the Drexel Autonomous Systems Lab (DASL)<sup>1</sup> if they could have their adult-size humanoid robot Jaemi Hubo throw the ceremonial first pitch at the second annual *Science Night at the Ballpark*. On April 28th, 2012 Hubo successfully threw the first pitch at the Philadelphia Phillies Vs. Chicago Cubs game, see Fig. 1.

Hubo was the first adult-size humanoid robot to throw the first pitch at a Major League Baseball game. This document describes how this was done via the analyses/tests of three different approaches and the resulting final design. Section II gives a brief introduction to work already done in the field as well as states the requirements for the pitch. Section III describes the three different methods tested where: Section III-A discusses the balancing methods and criteria used. Section III-B describes the human-robot kinematic mapping approach that uses a motion capture system to capture a human’s throwing motion then mapping that to an adult-size humanoid robot. Section III-C describes a fully automated approach that uses the sparse reachable map (SRM) to provide



Fig. 1. Hubo successfully throwing the first pitch at the second annual Philadelphia Science Festival event Science Night at the Ball Park on April 28th, 2012. The game was between the Philadelphia Phillies and the Chicago Cubs and played at the Major League Baseball stadium Citizens Bank Park. The Phillies won 5-2

viable full body throwing trajectories with the desired end effector velocity[1]. Section III-D describes the final method explored which is based on key-frame trajectories. Section IV compares the tests and analyses of each of the methods. Section V describes the final design in detail and the modifications needed to make the robot’s pitch reliable. Finally Section VI gives final thoughts and possible improvements for future years.

### II. BACKGROUND AND OBJECTIVES

The primary objective is to have our humanoid robot Jaemi Hubo throw a regulation Major League Baseball ball from the pitchers mound across home plate, a distance of 60.5 feet (18.4m). The regulation Major League Baseball ball has a circumference between  $9 - 9\frac{1}{4}$  inches (229-235mm) and weights  $5 - 5\frac{1}{4}$  ounces (142-149g) grams[2]. When children

<sup>1</sup>Drexel Autonomous Systems Lab: <http://dasl.mem.drexel.edu>

are asked to throw the first pitch it is typical for them to stand halfway between the pitchers mound and home plate. The robot used to throw the pitch, Jaemi Hubo, stands 130cm tall, the average height of a ten year old child. To properly fit the stature of the robot the pitch will be given from half the regulation distance. Using the well known projectile motion formulation it is determined that the robot must have an end effector velocity of  $9.47 \frac{m}{s}$  at  $45^\circ$  when it releases the ball in order for it to cross the plate.

Completing this objective with a humanoid robot consists of two major parts: 1) end-effector velocity control and 2) balance/stabilization. There are many examples of throwing/pitching machines made by commercial companies such as Louisville Slugger<sup>TM</sup>, Jugs<sup>TM</sup>, and Atec<sup>TM</sup> to name a few. These devices typically contain one to two fly wheels that the ball travels through in order to be launched or a spring loaded arm that is compressed and released. None of these robots are humanoid or bipedal. All of these devices are well planted to the ground to ensure stability.

Robots designed for throwing come in many shapes and sizes depending on the objective. 2-DOF mechanisms are able to throw in  $R^3$  space with the correct kinematic structure. Visual feedback was used in the basketball throwing robot ( $\leq 7$  DOF) by Hu et al. [3] achieving accuracy an of 99% at distances  $\leq 3m$ . This robot was fixed to the ground to guarantee stability. The PhillieBot<sup>2</sup> made by the GRASP Lab at the University of Pennsylvania was the robot that threw the first pitch at the first annual Philadelphia Science Festival *Science Night at the Ballpark* in 2011. The PhillieBot consisted of a  $\leq 7$  DOF arm with a pneumatic wrist actuator to increase end-effector velocity at the release point. The arm was attached to wheeled mobile platform. Kim et al. [4], [5] takes the research to the next level with finding optimal overhand and sidearm throwing motions for a high degree of freedom humanoid computer model. The model consists of 55-DOF and is not fixed to mechanical ground or a massive base. Motor torques are then calculated to create both sidearm and overhand throws that continuously satisfies the zero-moment-point stability criteria [6].

The highly articulated 40-DOF adult size humanoid robot Jaemi Hubo (Fig. 2) is the platform focused on in this work. Jaemi Hubo is a high-gain, position-controlled biped humanoid robot weighing 37kg and standing 130cm tall. It is designed and made by Dr. Jun-Ho Oh director of the Hubo Lab at the Korean Advanced Institute of Science and Technology (KAIST). Jaemi has been located at the Drexel Autonomous Systems Lab (DASL) at Drexel University since the Fall of 2008. DASL has extensive experience with the Jaemi Hubo KHR-4 platform in key areas needed to complete this work. Balancing was explored when developing a real-time zero moment point (ZMP) preview control system for stable walking [7]. A full-scale safe testing environment designed for experiments with Jaemi Hubo was created using DASL's Systems Integrated Sensor Test Rig (SISTR) [8]. Additionally

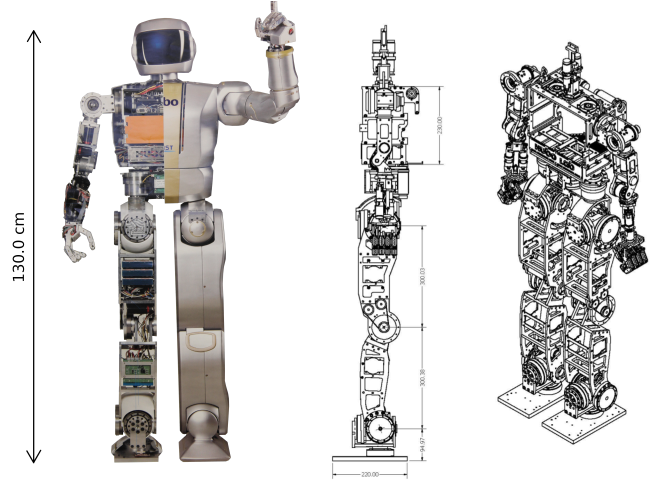


Fig. 2. Jaemi Hubo is a 130cm tall 37kg 40-DOF highly articulated, high-gain position controlled, adult-size humanoid robot.

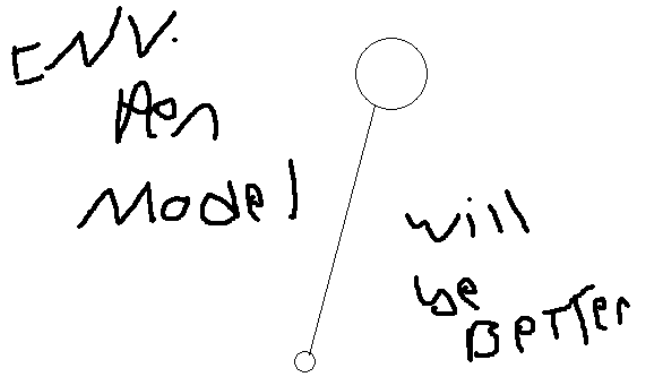


Fig. 3. Hubo modeled as a single inverted pendulum with COM located a distance  $L$  from

all algorithms are able to be tested on miniature and virtual versions of Jaemi Hubo prior to testing on the full-size humanoid robot through the creation of a surrogate testing platform for humanoid robots [9].

### III. METHODOLOGY

#### A. Balance and Stability

Each of the methods used have to be stable through the motion in order for the system to be stable (i.e. not to fall down). The well known zero-moment-point (ZMP) criteria is what each method must adhere to in order to stay statically stable[10]. To handle perturbation an active balance controller was added. The active balance controller is applied on top of the pre-defined trajectories. The Hubo is modeled as a single inverted pendulum with the center of mass (COM) located at length  $L$  from the ankle. The compliance of the robot is composed of a spring  $K$  and a damper  $C$ , see Fig. 3. An IMU located at the COM gives the measured orientation.

<sup>2</sup>PhillieBot Video: <http://youtu.be/Shld-vZ-ZEY>

The dynamic equation of the simplified model is assumed to be the same in both the sagittal and coronal plane.

$$mL^2\ddot{\theta} + C\dot{\theta} - Ku = 0 \quad (1)$$

This can be linearized and made into the transfer function:

$$G(s) = \frac{\Theta(s)}{U(s)} = \frac{\frac{K}{mL^2}}{s^2 + \frac{C}{mL^2}s + \frac{K-mgL}{mL^2}} \quad (2)$$

Prior work on the model and controller for the Hubo by Cho et. al. calculated  $K = 753 \frac{Nm}{rad}$  and  $C = 18 \frac{Nm}{sec}$  using the free vibration response method[11].

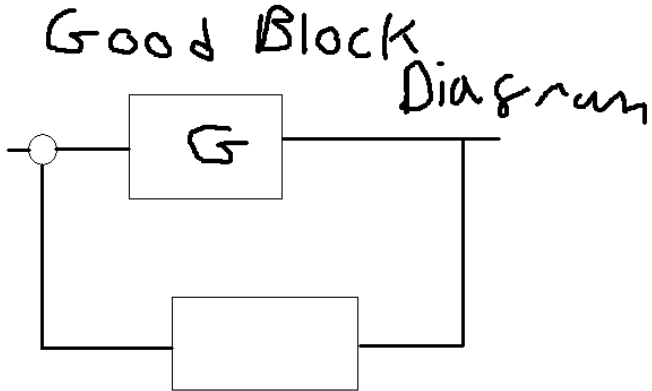


Fig. 4. Hubo successfully throwing the first pitch at the second annual Philadelphia Science Festival event Science Night at the Ball Park on April 28th, 2012. The game was between the Philadelphia Phillies and the Chicago Cubs and played at the Major League Baseball stadium Citizens Bank Park. The Phillies won 5-2

The control law is as follows

$$\theta_n^x = \theta_t^x + (K_p^x + sK_d^x) \left( \sum \theta_t^x - \theta_c^x \right) \quad (3)$$

Where  $\theta_t$  is the desired trajectory of the lower body (pitch or roll) and  $x$  denotes pitch or roll.  $\theta_c$  is the orientation of the center of mass in the global frame.  $\theta_n$  is the resulting trajectory.  $K_p$  and  $K_d$  are the proportional and derivative gains. The resulting control allows for a stable stance even with perturbations from upper body motions.

#### B. Human to Humanoid Robot Kinematic Mapping

Motion capture (MoCap) systems are commonly used to record high degree of freedom human motion. Athletic trainers in baseball, football and cycling use motion capture to analyze and improve throwing and lower limb motions[12], [13], [14], [15]. MoCap systems are also used to generate human-like motions and map those motion to humanoid robots[16], [17]. Fig. 5 shows the Hubo's kinematic structure (left) and the human (MoCap) kinematic structure(left). The human has 3-DOF at each joint while the humanoid robot has limited DOF at each corresponding joint. Some of the challenges

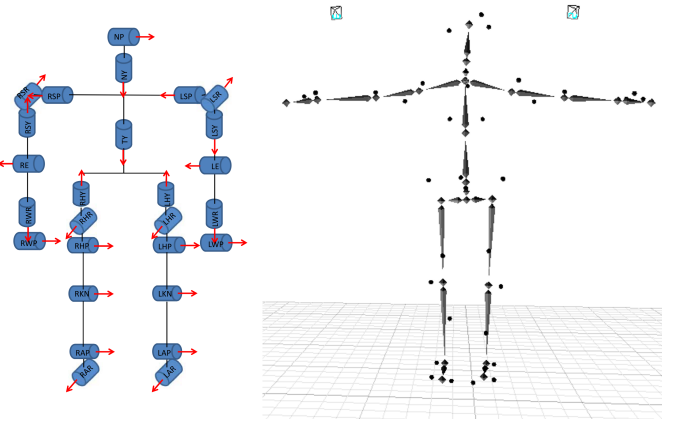


Fig. 5. Left: Jaemi Hubo joint order and orientation using right hand rule. Right: Motion capture model of human figure

in mapping between the human kinematic structure (from MoCap) to a humanoid robot's kinematic structure are:

- The difference in the total degree of freedom (DOF).
- The difference in the kinematics descriptions.
- The different Kinematic constraints.

Stefan et. al.[18] uses an intermediate model (Master Motor Map) to decouple motion capture data for further post-processing tasks. Our approach is to: a) Choose a set MoCap model. b) Perform motions where the pitch motions are decoupled (roll and yaw stay constant), avoids singularities and robot joint position limitations. c) Combine joint values for near by joints (reduce the model to the same DOF as the robot). d) Some tests require the addition of static offsets to joints to ensure the zero-moment-point (ZMP) criteria is satisfied as stated in Section III-A

To test this method we used a human subject to throw a ball using upper and lower body movements. All motions were in the sagittal plane to keep pitch joints decoupled. To avoid the robot's joint limit of  $\pm 180^\circ$  an underhand throwing motion was used. Fig. 6 shows the human throwing the ball and the robot throwing the ball to the mapped motion of the human.

To ensure balance throughout the motion the balance controller as described in Section III-A was applied and the static ZMP criteria was checked for the entire trajectory. The human subject threw the ball approximately eight feet (244cm). The mapping of the latter motion caused the robot to throw the ball approximately five feet (152cm). The discrepancy comes from the proportional difference in limb length from the human to the robot. A side by side video of the human and the robot throwing the ball is available for viewing on the this paper's homepage<sup>3</sup>.

#### C. Throwing Using Sparse Reachable Map

A Sparse Reachable Map (SRM) is used to create a collision free trajectories while having the end-effector reach a desired velocity as described in Lofaro et. al.[1]. The SRM has been shown to be a viable method for trajectory generation for

<sup>3</sup>MoCap to Robot (Video): <http://danlofaro.com/Humanoids2012/#mocap>



Fig. 6. Left: Human frame by frame throwing underhand in sagittal plane. Right: Throwing motion mapped to humanoid robot.

high degree of freedom, high-gain position controlled robots. This remains true when operating without full knowledge of the reachable area as long as a good collision model of the robot is available. The end-effector velocity (magnitude and direction) is specified as well as a duration of this velocity. The SRM is created by making a sparse map of the reachable end-effector positions in free space and the corresponding poses in joint space by using random sampling in joint space and forward kinematics. The desired trajectory in free space is placed within the sparse map with the first point of the trajectory being a known pose from the original sparse map.

$$L_d(0) \in SRM \quad (4)$$

$L_d(0)$  is known both in joint space and in free space. The Jacobian Transpose Controller method of inverse kinematics as described by Wolovich et al.[19] is then used to find the subsequent joint space values for the free space points in the trajectory.

$$q_1 = q_0 + \dot{q}_0 = q_0 + k J^T e|_{x_0}^{x_1} \quad (5)$$

Where  $q_0$  and  $x_0$  is the current pose and corresponding end-effector position respectively.  $q_1$  is the next pose for the next desired end-effector position  $x_1$ . Each desired end-effector position  $x$  must be within a euclidean distance  $d$  (user defined) from any point in the SRM.

$$\min(|x - SRM|) < d \quad (6)$$

If one of the points in  $x$  fails this criteria a new random point is chosen for  $L_d(0)$  and the process is repeated.

Each pose in the trajectory is checked against the collision model to guarantee no self-collisions. The collision model is based on the OpenRAVE model of the Hubo platform called OpenHUBO, see Fig 7.

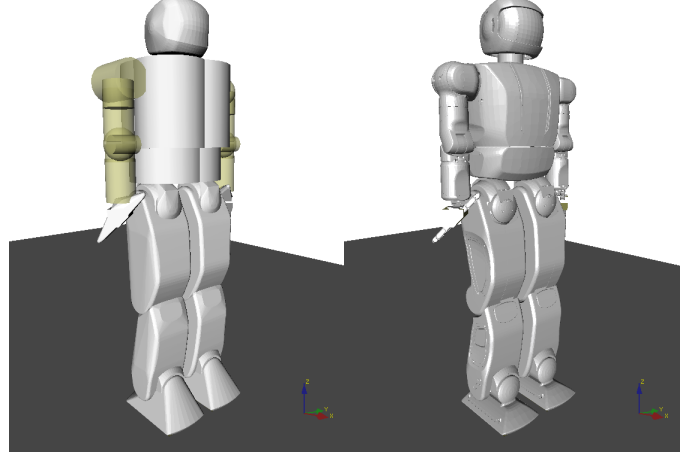


Fig. 7. OpenHUBO - OpenRAVE model of Hubo KHR-4. Left: Collision Geometry. Right: Model with protective shells[1].

The commanded trajectory produces the desired velocity of 4.9m/s at 60°. This was then tested on the OpenHUBO and on the Jaemi Hubo platform, Fig 8 and Fig 9 respectively.

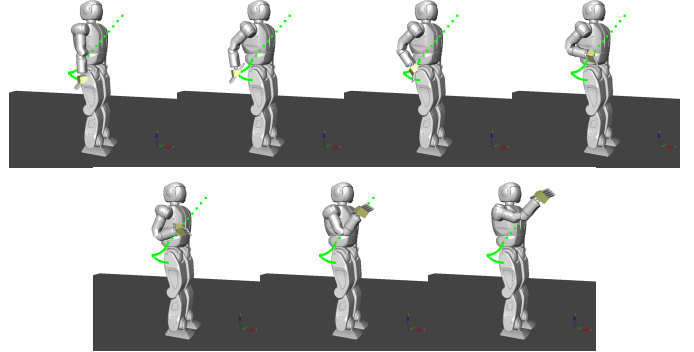


Fig. 8. OpenHUBO running the throwing trajectory immediately after the setup phase is completed.  $x_0$  is top left. Frames are read left to right and have a  $\Delta t$  of 0.15s[1]

To ensure balance throughout the motion the balance controller as described in Section III-A was applied and the static ZMP criteria was checked for the entire trajectory. This method worked as desired. In approximately 10% of the tests one or more joints would over torque and shutdown. This is due to the system not taking the robots power limitations into account.

#### D. Key-Frame Motion

Key-frame motion profiles for humanoid robots borrows from the animation industries' long used animation techniques. When making an animation the master animator will create the character in the most important (or key) poses. The apprentice animators will draw all of the frames between the key poses. We borrowed this technique when we: posed the robot in the desired pose, record the values in joint space, and make a smooth motion between poses. In place of the

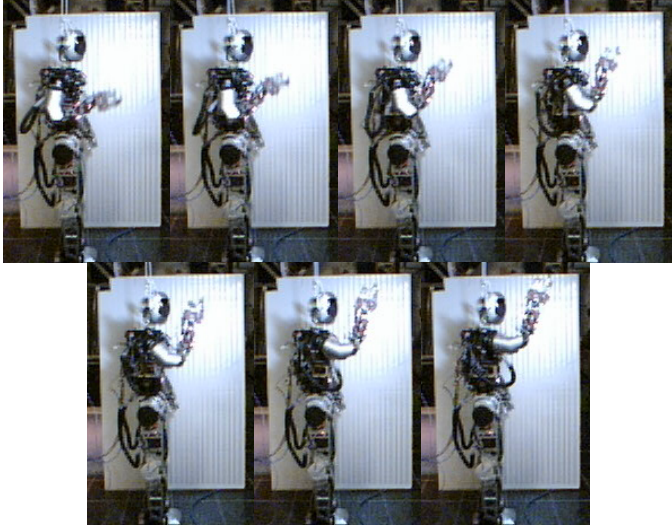


Fig. 9. Jaemi Hubo running the throwing trajectory immediately after the setup phase is completed.  $x_0$  is top left. Frames are read left to right and have a  $\Delta t$  of 0.15s[1]



Fig. 10. OpenHUBO moving between key-frames (green) using interpolation methods.

apprentice animators, forth order interpolation methods were used to make smooth trajectories between poses. Forth order interpolation was used in order to limit the jerk on each of the joints. The resulting trajectory is a smooth well defined motion as seen in Fig. 10.

To ensure balance throughout the motion the balance controller as described in Section III-A was applied and the static ZMP criteria was checked for the entire trajectory. The resulting end effector velocity was  $4.8 \frac{m}{s}$  at the release point. Fig. 11 shows the plot of the magnitude of the end effector's velocity. The release point is marked. It should be noted that the release point has the velocity vector at an elevation of  $40^\circ$  from the ground.

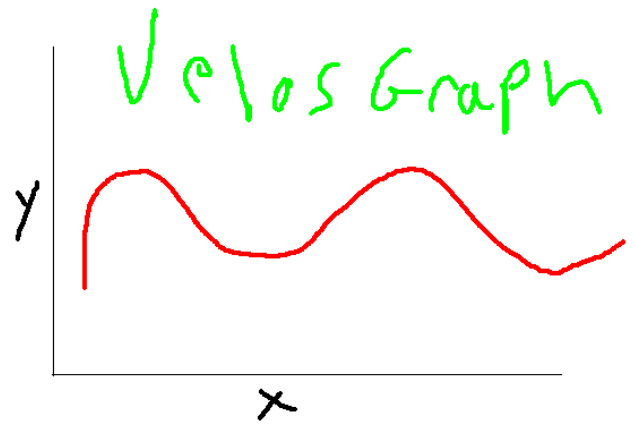


Fig. 11. key-frame throw velocity graph

TABLE I  
COMPARISON BETWEEN THE THREE DIFFERENT METHODS OF  
END-EFFECTOR (EEF) VELOCITY CONTROL: HUMAN-ROBOT JOINT  
MAPPING (MoCap), SRM BASED AND KEY-FRAME

	EEF Velocity ( $\frac{m}{s}$ )	Joint Failure (%)	Throw Overhand (y/n)	Stable (y/n)
MoCap	4.0	0	n	y
SRM	4.9	10	y	y
Key-Frame	4.8	0	y	y

#### IV. METHOD COMPARISON

All three methods described were shown to be stable during the throwing motion and can successfully throw a baseball. Table I shows the end-effector (EEF) velocity, joint failure rate, overhand or underhand throwing and stability of the three different methods of end-effector velocity control used in this paper human-robot joint mapping (MoCap), SRM based and key-frame.

The SRM technique worked well however the large jerk on each of the joints created large torques caused the motor controller to over torque/current and shutdown 10% of the time. The pitch needs to work 100% of the time thus this method is not well suited for the event. Both the human-robot joint mapping via MoCap and key-frame based methods consistently worked and stayed stable. A secondary objective is to have the throwing motion be overhand like a standard Major League Baseball pitcher. Due to the constraints placed on the joint mapping of the MoCap method in Section III-B an over arm throw would be impossible to perform due to the robot's  $\pm 180^\circ$  joint limitations. The key-frame method was chosen as the method to throw the ball. Section V describes the modifications to the system to allow it to reliably throw the pitch the desired distance.

#### V. FINAL DESIGN

The final goal is to have an end-effector velocity of  $9.47 \frac{m}{s}$  at  $45^\circ$ . The key-frame method was tested to throw at  $4.8 \frac{m}{s}$ .

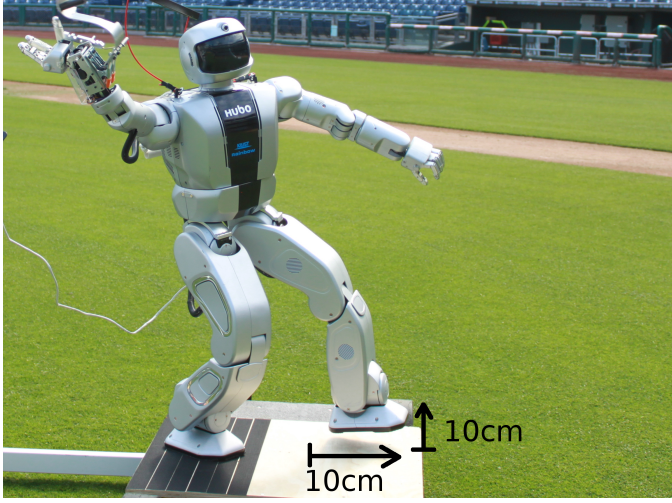


Fig. 12. Hubo stepping 10cm up and forwards increasing the end effector velocity by  $2.3 \frac{m}{s}$ .

To increase the end-effector velocity the upper body motion was kept unchanged but the lower body added a stepped up with the left foot, pushed forward with the right foot and stepped forward 10cm with the left. Stepping with your non-dominant foot, and pushing with your dominant, when throwing overhand is common practice to increase the distance you can throw a ball. Jaemi Hubo throws with its right hand and steps with its left. This increased the end-effector velocity from  $4.8 \frac{m}{s}$  to  $7.1 \frac{m}{s}$ . Fig. 12 shows the stepping motion of the robot.

The addition of pushing off with the right foot and stepping forward introduced two problems. 1) The ZMP criteria is not satisfied throughout the motion and 2) the right foot would slip when pushing its body forward. To remedy this hook and loop was placed on the bottom of the right foot and on the platform where Hubo would throw from. This did not permanently attach the robot to the platform but it did allow for more friction between the foot and the ground. This allowed the balancing controller to function adequately for the short step and maintain stability. The platform was added to ensure a more consistent ground for the robot to balance on than the baseball field can inherently provide.

An additional  $2.5 \frac{m}{s}$  was needed to give a proper throw. Borrowing from the GRASP Lab and their high powered pneumatic wrist on their PhillieBot, a spring loaded mechanism was added to Hubo's wrist, see Fig. 13. The addition of this mechanism allowed the robot to achieve an end-effector velocity magnitude of  $10 \frac{m}{s}$ . Fig. 14 shows a frame overlay of the the Hubo throwing a regulation baseball 10m (32.8feet). Fig. 1 shows the same throw at Citizens Bank Park on April 28<sup>th</sup>, 2012.

## VI. CONCLUSION

The creation of a reliable humanoid throwing method was completed. This allowed the Hubo to complete its goal of becoming the first adult-size humanoid robot to throw the

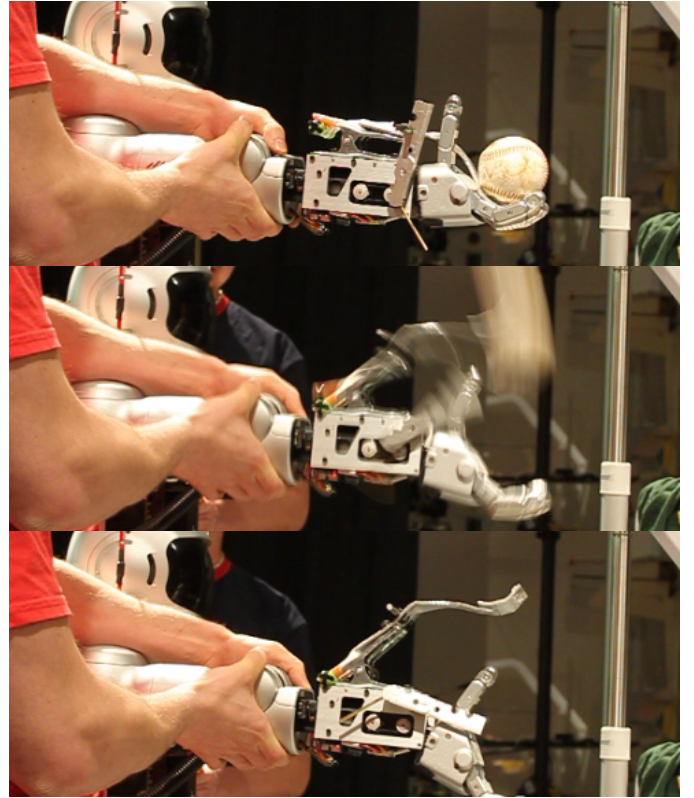


Fig. 13. Spring loaded mechanism test launching the baseball. Top: Pre-launch. Middle: Launch. Bottom: Pos-launch. The mechanism added  $3.0 \frac{m}{s}$  to the end-effector velocity at its release point.

first pitch at a Major League Baseball game. Three methods of creating a viable throw were explored and tested: human-robot mapping via motion capture, sparse reachable map based trajectory generation and a key-frame based method. Though the key-frame based method was the simplest it also proved to be the most viable. The balancing controller ensured stability of the system throughout the throw. With the addition of a high powered wrist and having the robot step forward when it throws created conditions for a successful and reliable pitch. More information and media about this event is available on this papers home page <http://danlofaro.com/Humanoids2012/>

## ACKNOWLEDGMENT

This project was supported by the Drexel Autonomous Systems Lab (DASL), the Music Entertainment Technology Lab (MET)<sup>4</sup>, and the National Science Foundation via the two grants; Partnerships for International Research and Education (#0730206) and Major Research InfrastructureRecovery and Reinvestment (#CNS-0960061). Special thanks for organization and technical assistance goes to the Philadelphia Science Festival, Robert Ellenberg and Roy Gross. The robot platform used was Hubo, designed and created by our partner Dr. Jun-Ho Oh, Department of Mechanical Engineering, Korean Advanced Institute of Science and Technology, Daejeon, South Korea.

<sup>4</sup>Music Entertainment Technology Lab: <http://music.ece.drexel.edu>



Fig. 14. Frame overlay of the Hubo throwing overhand a distance of 10m (32.8 feet) with a release angle of  $40^\circ$  and a tip speed of 10m/s. Captured at 20fps with a shutter speed of 1/30 sec. Each of the white dashes of in the image is the actual baseball as picked up by the video camera.

## REFERENCES

- [1] D. Lofaro, R. Ellenberg, P. Oh, and J. Oh, "Humanoid throwing: Design of collision-free trajectories with sparse reachable maps," in *Intelligent Robots and Systems (IROS), 2012 IEEE/RSJ International Conference on*, oct. 2012.
- [2] S. Alderson, B. Gorman, J. Schuerholz, B. Beban, J. John McHale, J. L. Solomon, R. Carew, T. Ryan, and B. Stoneman. (2012, Jun.) Official rules of major league baseball. [Online]. Available: [http://mlb.mlb.com/mlb/official\\_info/official\\_rules/foreword.jsp](http://mlb.mlb.com/mlb/official_info/official_rules/foreword.jsp)
- [3] J.-S. Hu, M.-C. Chien, Y.-J. Chang, S.-H. Su, and C.-Y. Kai, "A ball-throwing robot with visual feedback," in *Intelligent Robots and Systems (IROS), 2010 IEEE/RSJ International Conference on*, oct. 2010, pp. 2511 –2512.
- [4] J. Kim, "Motion planning of optimal throw for whole-body humanoid," in *Humanoid Robots (Humanoids), 2010 10th IEEE-RAS International Conference on*, dec. 2010, pp. 21 –26.
- [5] J. H. and Kim, "Optimization of throwing motion planning for whole-body humanoid mechanism: Sidearm and maximum distance," *Mechanism and Machine Theory*, vol. 46, no. 4, pp. 438 – 453, 2011. [Online]. Available: <http://www.sciencedirect.com/science/article/pii/S0094114X10002168>
- [6] M. Vukobratovic, "How to control artificial anthropomorphic systems," *Systems, Man and Cybernetics, IEEE Transactions on*, vol. 3, no. 5, pp. 497 –507, sept. 1973.
- [7] Y. Jun, R. Ellenberg, and P. Oh, "Realization of miniature humanoid for obstacle avoidance with real-time zmp preview control used for full-sized humanoid," in *Humanoid Robots (Humanoids), 2010 10th IEEE-RAS International Conference on*, dec. 2010, pp. 46 –51.
- [8] R. Ellenberg, R. Sherbert, P. Oh, A. Alspach, R. Gross, and J. Oh, "A common interface for humanoid simulation and hardware," in *Humanoid Robots (Humanoids), 2010 10th IEEE-RAS International Conference on*, dec. 2010, pp. 587 –592.
- [9] R. Ellenberg, D. Grunberg, P. Oh, and Y. Kim, "Using miniature humanoids as surrogate research platforms," in *Humanoid Robots, 2009. Humanoids 2009. 9th IEEE-RAS International Conference on*, dec. 2009, pp. 175 –180.
- [10] M. Vukobratovic and J. Stepanenko, "On the stability of anthropomorphic systems," *Mathematical Biosciences*, vol. 15, no. 12, pp. 1 – 37, 1972.
- [11] B.-K. Cho, S.-S. Park, and J. ho Oh, "Controllers for running in the humanoid robot, hubo," in *Humanoid Robots, 2009. Humanoids 2009. 9th IEEE-RAS International Conference on*, dec. 2009, pp. 385 –390.
- [12] S. Fleisig, R. F. Escamilla, J. R. Andrews, T. Matsuo, Y. Satterwhite, and S. W. Barrentine, "Kinematic and kinetic comparison between baseball pitching and football passing," *Journal of Applied Biomechanics*, vol. 12, pp. 207–224, 1996.
- [13] W. Barrentine, T. Matsuo, R. F. Escamilla, G. S. Fleisig, and J. R. Andrews, "Kinematic analysis of the wrist and forearm during baseball pitching," *Journal of Applied Biomechanics*, vol. 14, no. 1, pp. 24–39, jan 1998.
- [14] Y. Mochizuki, T. Matsumoto, S. Inokuchi, and K. Omura, "Computer simulation of the effect of ball mass and shape to upper limb in baseball pitching," *Theoretical and Applied Mechanics*, vol. 47, pp. 283–292, 1998.
- [15] A. Uesaki, Y. Mochizuki, T. Matsuo, K. Hashizume, K. Omura, and S. Inokuchi, "Computer simulation for dynamics analysis of pedaling motion on lower limbs in a racing cycle," *Theoretical and Applied Mechanics*, vol. 48, pp. 197–205, 1999.
- [16] Q. Huang, Z. Peng, W. Zhang, L. Zhang, and K. Li, "Design of humanoid complicated dynamic motion based on human motion capture," in *Intelligent Robots and Systems, 2005. (IROS 2005). 2005 IEEE/RSJ International Conference on*, aug. 2005, pp. 3536 – 3541.
- [17] S. Pollard, J. Hondgins, M.J. Riley, and C. Atkeson, "Adapting human motion for the control of a humanoid robot," in *In Proc. of IEEE International Conference on Robotics and Automation*, 2002.
- [18] S. Gaertner, M. Do, T. Asfour, R. Dillmann, C. Simonidis, and W. Seemann, "Generation of human-like motion for humanoid robots based on marker-based motion capture data," *Robotics (ISR), 2010 41st International Symposium on and 2010 6th German Conference on Robotics (ROBOTIK)*, pp. 1 –8, june 2010.
- [19] W. A. Wolovich and H. Elliott, "A computational technique for inverse kinematics," in *Decision and Control, 1984. The 23rd IEEE Conference on*, vol. 23, dec. 1984, pp. 1359 –1363.